

Corrosion of Iron in Sulfur Dioxide at 0.1 MPa

J. Gilewicz-Wolter* and Z. Żurek†

Received February 14, 1994; revised April 24, 1995

The reaction of iron with sulfur dioxide at 0.1 MPa and 1073 K was studied. The composition and morphology of the scales, transport phenomena occurring in the growing scales, and kinetics of the process were investigated. Scanning electron microscopy and various techniques of X-ray analysis were used. The transport phenomena were studied by marker and by radiotracer techniques. The scales were composed of sulfide and oxides and grew by the outward diffusion of metal. It was concluded that the process initially took place through the reaction of iron with sulfur dioxide molecules. During the next stage of the process the reaction with sulfur dioxide molecules as well as with oxygen molecules is possible.

KEY WORDS: iron; sulfur dioxide; oxidation; tracer.

INTRODUCTION

In high-temperature industrial systems metallic materials are often exposed to gases containing more than one oxidizing agent. Hot combustion gases contain a number of elements, such as oxygen, sulfur, carbon, and nitrogen, which can give rise to aggressive species. The corrosion of metals in such atmospheres is still insufficiently understood to predict the behavior of a given material under industrial conditions.

Many authors¹⁻¹⁰ who have studied the reaction of iron with sulfur dioxide agree that the scale formed at temperatures ranging between 773 K and 1173 K contains oxides and sulfide. However, the iron sulfide is unstable

*The Faculty of Physics and Nuclear Techniques, University of Mining and Metallurgy, al. Mickiewicza 30, 30-059 Kraków, Poland.

†Institute of Inorganic Chemistry and Technology, Cracow University of Technology, ul. Warszawska 24, 31-155 Kraków, Poland.

under these reaction conditions because the partial pressure of sulfur, which is a product of the dissociation of sulfur dioxide, is lower than the dissociation pressure of iron sulfide. The structure of the scale depends on sulfur dioxide pressure and the reaction temperature.

The presence of the sulfide in the scale facilitates the outward transport of metal, thereby accelerating corrosion. Thus, various papers have concentrated on the simultaneous formation of oxide and sulfide. According to Birks^{1,2} the formation of the oxide, being a stable product under the reaction conditions, lowers the partial pressure of oxygen to the value of the oxide-dissociation pressure, in accordance with the equilibrium:



This causes the sulfur partial pressure to increase and gives the possibility of sulfide formation. Sulfide formation, in turn, causes the sulfur pressure to decrease, with a simultaneous increase of the oxygen pressure. These local variations of pressures may result in the formation of sulfide on the surface of the scale and inside it when inward transport of SO_2 takes place.

Rahmel^{3,4} suggested another mechanism for this process. The sulfide may be formed inside the scale due to the solubility of sulfur in the oxide and its diffusion as well as to the inward transport of sulfur dioxide molecules through microdiscontinuities in the scale. Oxide and sulfide may be formed simultaneously on the scale surface when diffusion from the gaseous phase or the reaction at the scale-gas interface is the rate-determining process. An excess of metal ions on the surface of the scale may react with any available reaction species which appears first on the surface.

According to Gesmundo^{6,7} and Luthra and Worrell^{11,12} the correct mechanism involves a reaction of the metal with sulfur dioxide molecules rather than those of sulfur and oxygen. This hypothesis was confirmed by experiments conducted by McAdam and Young.⁸

In this paper an attempt is made to explain the mechanism of scale formation on iron in a sulfur dioxide atmosphere at 0.1 MPa, based on tests of scale composition and structure at various stages of its formation, kinetics of the process, and radioisotope investigations of sulfur transport in the scale.

EXPERIMENTAL PROCEDURES

Investigations of the kinetics of oxidation of iron in sulfur dioxide at 0.1 MPa and temperatures 873 K, 973 K, 1073 K, and 1173 K were carried out. The composition of scales and their structure as well as the transport of reagents were studied at 1073 K only, thereby limiting the interpretation of results to this temperature. For kinetics experiments, samples of Armco

iron 30 mm in diameter and 2 mm thick were used. Their surfaces were prepared in a routine manner; i.e., they were first polished to a bright finish, then degreased in acetone and ethanol. The prepared samples were placed in the apparatus¹³ where the mass increase was measured with an accuracy of 10^{-5} g.

In the studies of the scale composition and structure, X-ray diffraction, an X-ray microanalyzer, and SEM were used. Transport of reactants were observed using samples of spectrally pure iron, produced by Johnson and Matthey. The surfaces of the samples were prepared as for the kinetics studies, except that the samples were first vacuum-annealed at 1273 K. The same samples were employed for studies of the scale composition and structure at 1073 K.

In the radiotracer experiments sulfur dioxide labeled with the sulfur radioisotope, sulfur-35, was used.

Tracer experiments were performed using the method of two-stage oxidation¹⁰; i.e., initially the reaction was carried out in natural sulfur dioxide and then in sulfur dioxide labeled with radioactive sulfur. This method makes it possible to detect the location of the radioactive sulfur in the nonradioactive part of the scale. The distribution of sulfur-35 was determined by autoradiography. The dark parts of the autoradiographs indicate the presence of the radioactive tracer.

RESULTS

Phase Composition and Morphology of Scales

Phases in the scale depend upon the oxidation time; after longer times (above 10 min) the scale consists of iron sulfide, wüstite, magnetite, and traces of hematite on the surface. At shorter oxidation times ($t < 10$ min) hematite was not observed. These phases are in agreement with the results obtained by other authors.^{6,7}

Near the metallic core an oxide-sulfide layer formed, which was covered with a compact oxide layer similar to the one obtained in oxygen.

Figures 1-5 are microphotographs of fractographs (a) and surfaces (b) of scales formed after 0.5 min, 1 min, 5 min, 20 min, and 4 hr (samples oxidized for the three shortest times were cooled in a stream of sulfur dioxide).

Scale formed over 0.5 min is porous and black. EDAX analysis of the inside of the scale and its outer surface showed the presence of sulfur.

Scale formed over 1 min is slightly different from the one obtained after 0.5 min of oxidation; i.e., the porous layer formed on the surface of the core is covered with a thin layer of brown-red scale. EDAX analysis of material from the surface indicated that traces of sulfur are present only in some places.

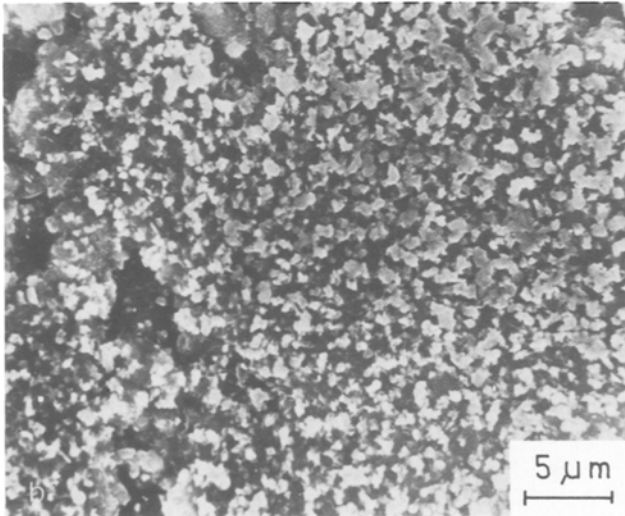
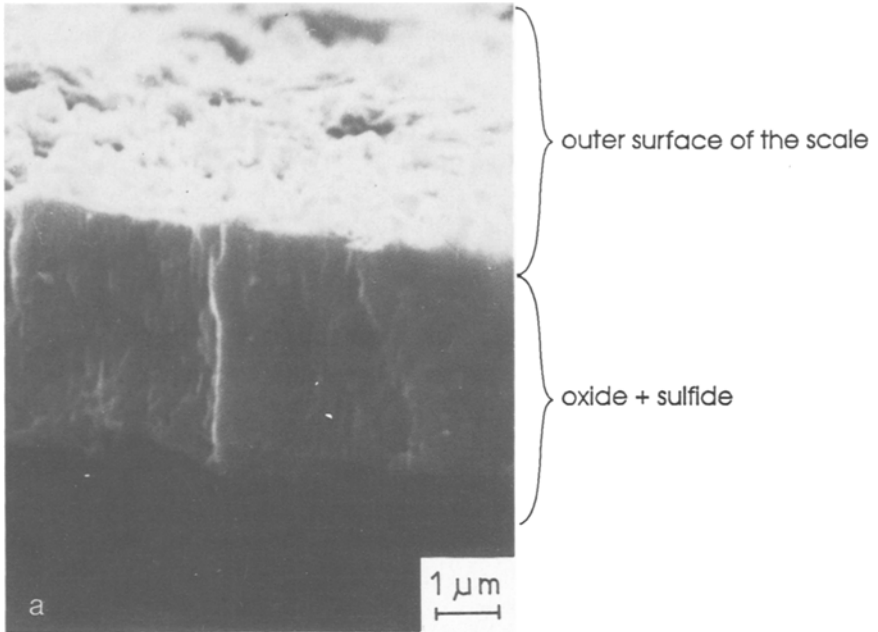


Fig. 1. SEM micrographs of the fracture (a) and surface (b) of the scale formed after $t = 0.5$ min at 1073 K in $P_{\text{SO}_2} = 10^5$ Pa.

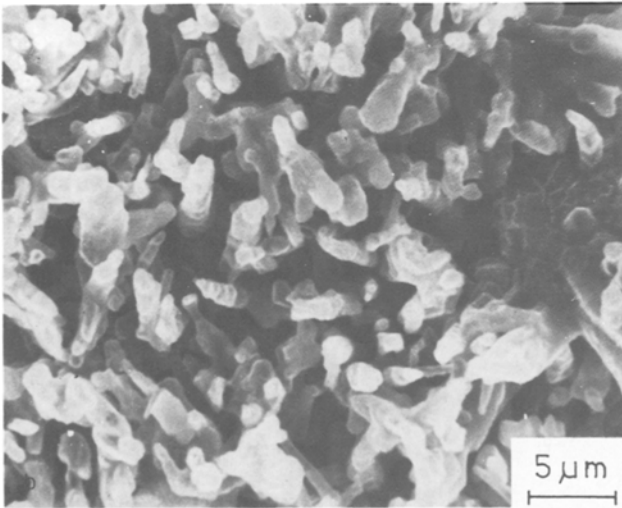
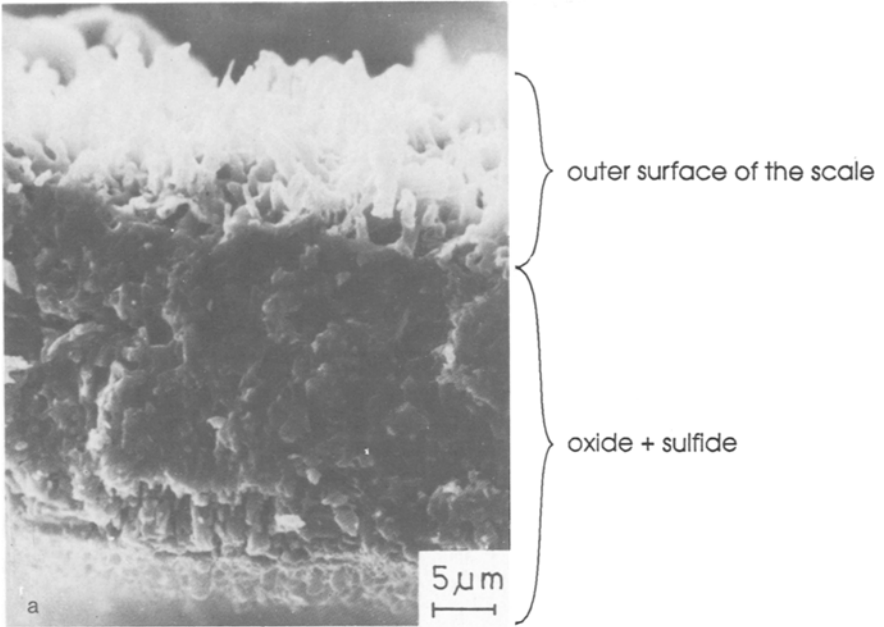


Fig. 2. SEM micrographs of the fracture (a) and surface (b) of the scale formed after $t = 1$ min at 1073 K in $P_{\text{SO}_2} = 10^5$ Pa.

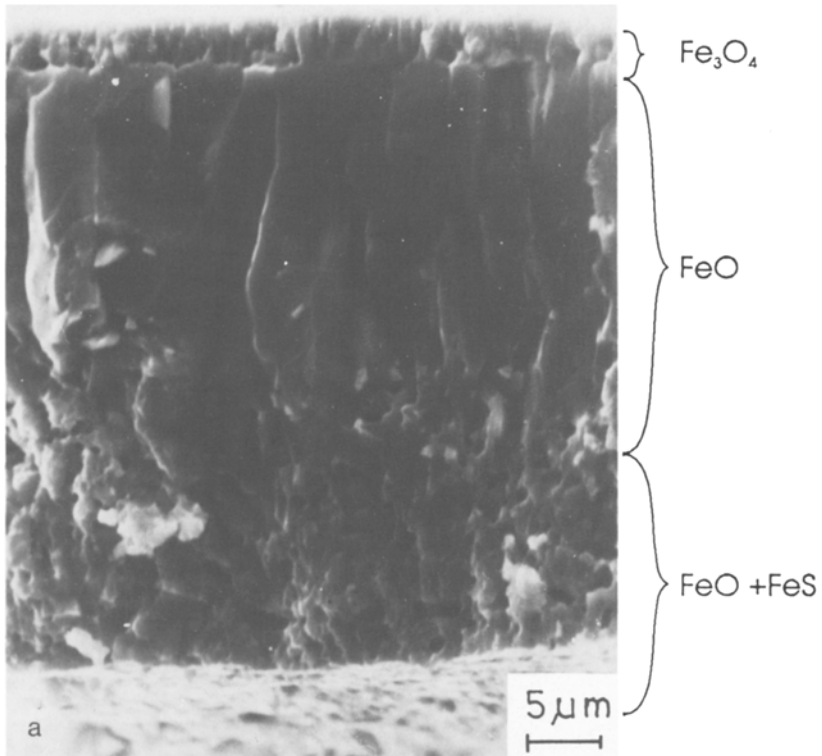


Fig. 3. SEM micrographs of the fracture (a) and surface (b) of the scale formed after $t = 5$ min at 1073 K in $P_{\text{SO}_2} = 10^3$ Pa.

Oxidation times longer than several minutes enhance the formation of a multilayer scale.

It follows from Figs. 4 and 5 that an increase in the reaction time causes only the growth of a compact oxide layer, whereas the thickness of the inner heterophase layer is practically unchanged. A thin compact magnetite layer with traces of hematite on the surface at the scale-gas interface formed.

The surfaces of samples oxidized for different times exhibit considerable differences in their morphology. The surfaces of samples oxidized for 0.5 min are covered with fine, loosely connected grains of iron sulfide and oxide. An increase of the oxidation time to 1 min causes the formation of longish forms resembling entangled fingers. As the oxidation time increases, the outer oxide layer becomes compact and its surface becomes smooth. Tiny crystallites forming a mosaic structure are characteristic of this surface. After a longer oxidation time (4 hr) the surface is slightly bumpy and no tiny crystallites are observed.

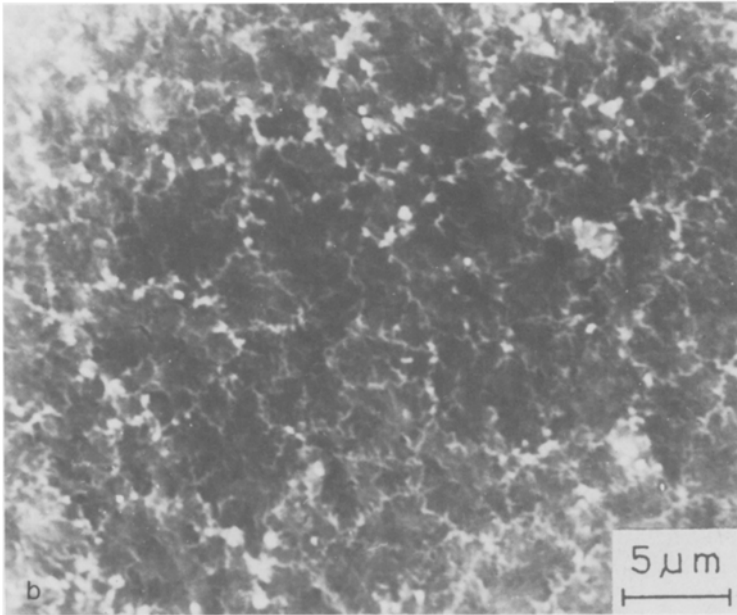


Fig. 3. Continued.

Kinetics of the Process

Figure 6 presents kinetics curves of oxidation of Armco iron in sulfur dioxide at 0.1 MPa at various temperatures. It follows from these curves that the process of iron oxidation under such conditions initially follows a linear and then a parabolic rate law. The duration of the linear process depends on the temperature.

Table I presents values of parabolic rate constants of iron oxidation under the above conditions. These values are compared with the parabolic rate constants for iron oxidation in pure oxygen.

Table II shows the rate constants for the initial stage of the process. These values have a considerable uncertainty due to the short times.

Transport of Reactants

Marker studies and the two-stage oxidation method, employing sulfur dioxide labeled with sulfur-35, were used. A Pt marker, placed on the metal surface before the reaction, was found at the metal-scale interface after the reaction. After reaction times of 10 or so hours, a very small amount of fine sulfide dust between the marker and core was observed.

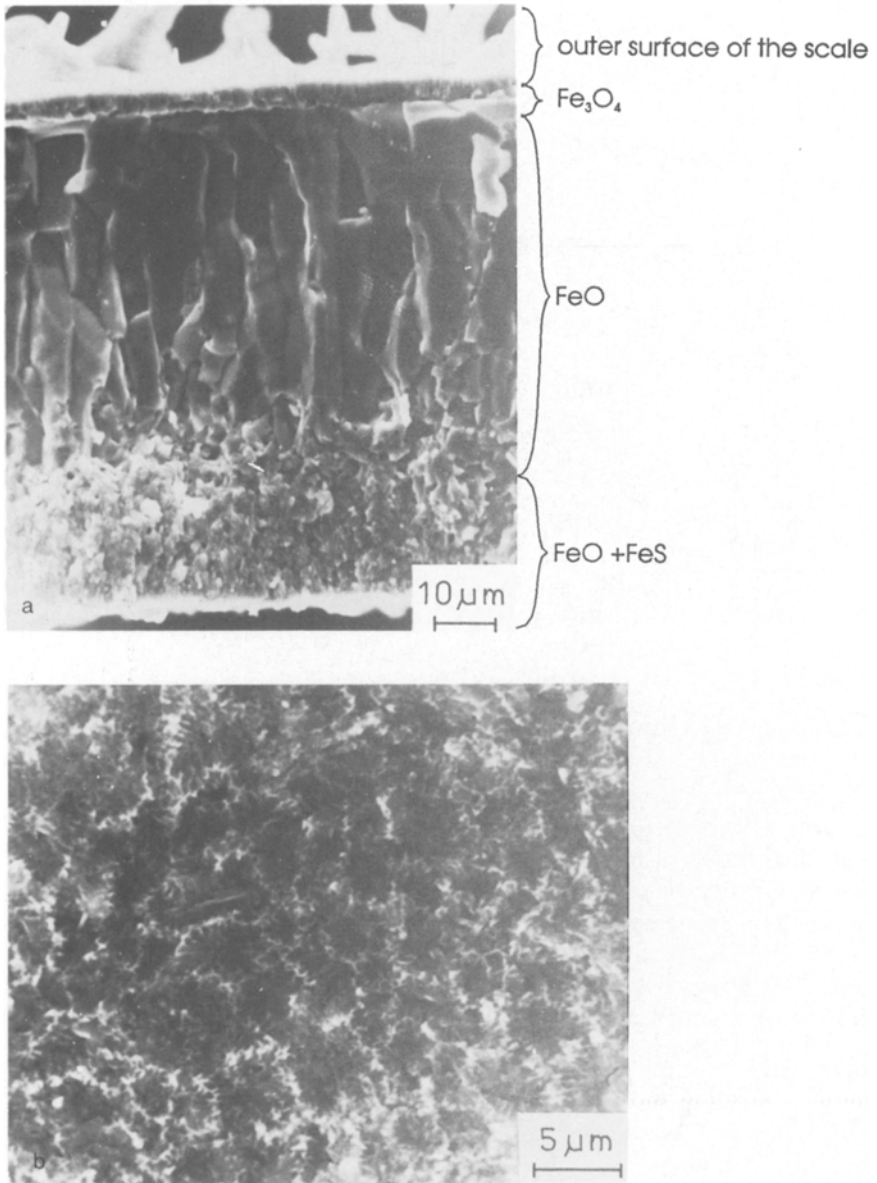


Fig. 4. SEM micrographs of the fracture (a) and surface (b) of the scale formed after $t = 20$ min at 1073 K in $P_{\text{SO}_2} = 10^5$ Pa.

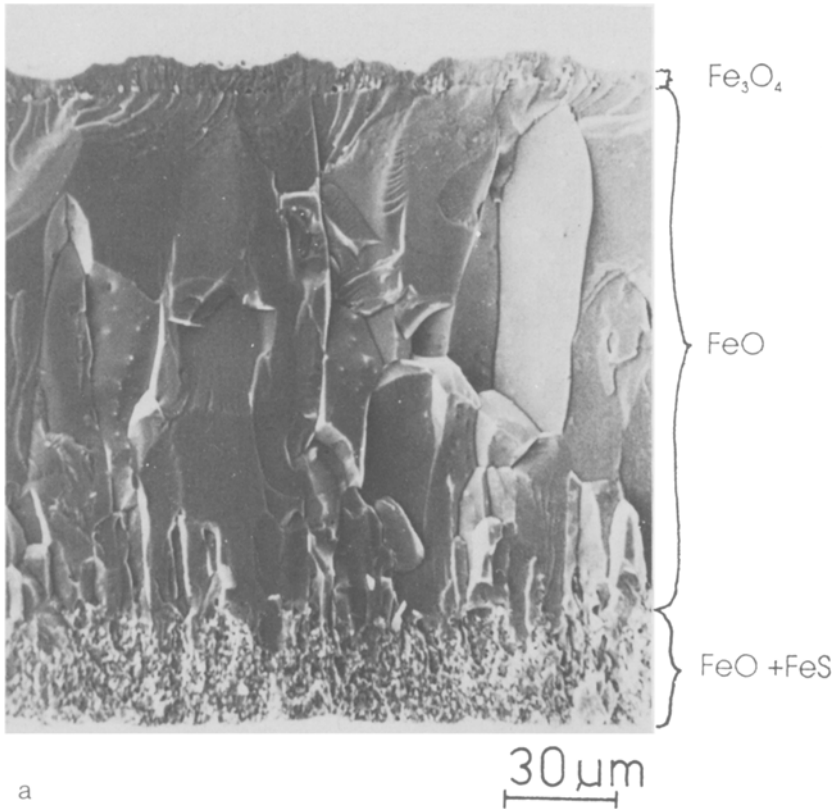


Fig. 5. SEM micrographs of the fracture (a) and surface (b) of the scale formed after $t = 240$ min at 1073 K in $P_{\text{SO}_2} = 10^5$ Pa.

Two types of radioisotope experiments were carried out: (1) The first stage of the reaction took place in sulfur dioxide, whereas the second occurred in sulfur dioxide labeled with sulfur-35. (2) The first stage of the reaction took place in sulfur dioxide labeled with ^{35}S , whereas the second occurred in natural sulfur dioxide.

In the first case no inward bulk diffusion of sulfur was observed. It has been found that after long oxidation times (16 hr in sulfur dioxide and 2 hr in sulfur dioxide labeled with ^{35}S) radioactive sulfur was present in the layer formed at the metal-scale interface in the corners of the sample (Fig. 7). After a longer reaction time in the radioactive environment (5 hr), ^{35}S was present in the whole layer formed in the metal-consumption zone (see Fig. 8).¹⁰ Based on the experiments in which the first stage of the reaction was

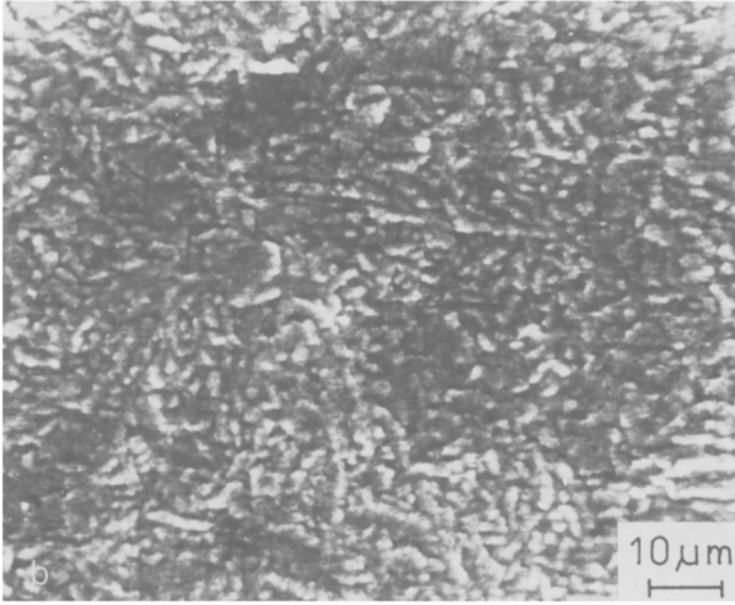


Fig. 5. Continued.

carried out in the radioactive gas and the second stage in the nonradioactive one, no sulfur transport toward the scale–gas interface was observed.

DISCUSSION

Figure 9 presents a phase-stability diagram of the iron–oxygen–sulfur system at 1073 K. The isobar for sulfur dioxide of 0.1 MPa has been marked on the diagram. Point A refers to pure sulfur dioxide, point C to the gas containing 10 Pa of oxygen (used in the experiments) taking into account reaction (1), and point B to equilibrium of reaction (1) and the following reaction of sulfur trioxide formation:



In the experiments no Pt catalyst was used, and the point corresponding to the real gas composition falls between points B and C. Figure 9 indicates that hematite is the equilibrium phase. Iron sulfide is unstable under these conditions, and its formation is not predicted.

The reaction rate in the initial stages is approximately constant. During the linear stage of the process an oxide–sulfide layer is formed. After a certain time the process begins to follow a parabolic law. At this stage the

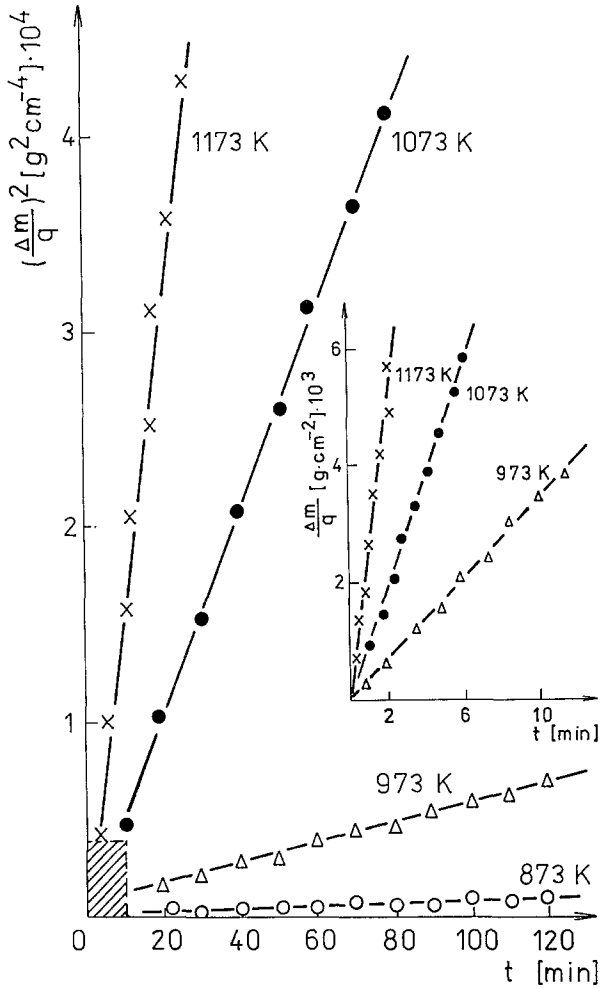


Fig. 6. Scaling kinetics of iron at 10^5 Pa of sulfur dioxide.

Table I. Values of Parabolic Rate Constants of Iron Oxidation in Sulfur Dioxide (this work) and Oxygen^{1,7,20} at 0.1 MPa

Temperature [K]	$k_p [g^2 cm^4 s^{-1}]$		Ref.
	SO ₂	O ₂	
873	1.2×10^{-9}	—	—
973	8.6×10^{-9}	6.5×10^{-9}	7
1073	8.5×10^{-8}	6.6×10^{-8}	1
1173	4.5×10^{-7}	3.4×10^{-7}	20

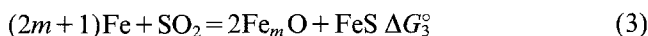
Table II. Values of Linear Rate Constants of Iron Oxidation in Sulfur Dioxide at 0.1 MPa

Temperature [K]	k_l [g cm ⁻² s ⁻¹]	Time of duration of linear process [min]
973	0.6×10^{-5}	8–10
1073	1.7×10^{-5}	6–8
1173	4.7×10^{-5}	1–2

surface is covered with a scale having the structure and composition identical to the one formed in oxygen.

Marker investigations have shown that outward iron diffusion is the main transport process and that the scale grows mainly at the scale–gas interface. The appearance of surfaces observed after 5 and 20 min of reaction seems to suggest that, during this stage, grain-boundary diffusion plays an important role. This is understandable, because a fine-crystallite scale is observed during this early stage of reaction.

The phases in the scale formed during the first minutes of the reaction are iron oxide and sulfide, despite the unfavourable thermodynamic conditions for sulfide formation. This result appears to support Gesmundo's hypothesis^{6,7} that the initial stage of the process follows the reaction

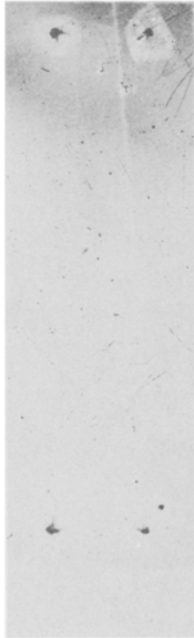
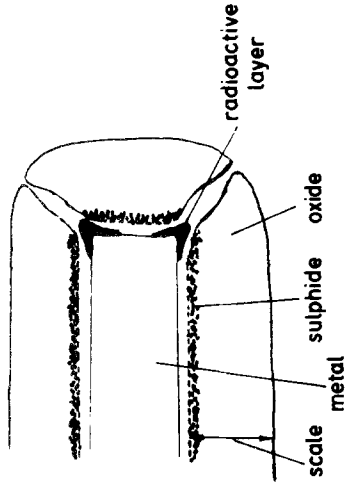


Oxide and sulfide form together by this reaction. Gesmundo was able to show that reaction (3) is the most important process in the formation of such scales. The lowest sulfur pressure required to form FeS is the dissociation pressure (at 1073 K, $P_{\text{S}_2} = 1.2 \times 10^{-4}$ Pa). The corresponding oxygen pressure established by the equilibrium (1) is higher than the dissociation pressure of FeO (at 1073 K, $P_{\text{O}_2} = 10^{-7}$ Pa). The maximum reaction rate is given by the rate of impingement of O₂ and S₂ molecules on the sample surface which can be calculated using the Hertz–Knudsen–Langmuir equation:

$$J(\text{X}_2) = p(\text{X}_2) \left[\frac{M}{2\pi RT} \right]^{1/2} \quad (4)$$

where $J(\text{X}_2)$ is the flux of gas molecules impinging on the surface of the sample, $p(\text{X}_2)$ is the gas pressure, M is the molecular weight of the gas, and T is the temperature.

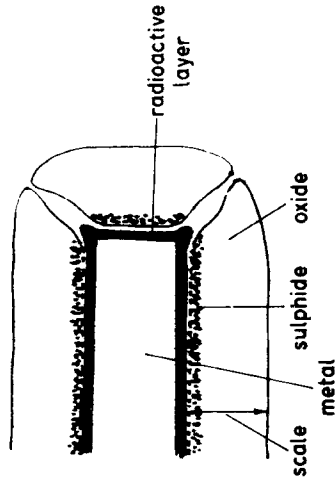
In our experimental conditions the total flux of oxygen and sulfur molecules, $J(\text{O}_2 + \text{S}_2)$, calculated from Eq. (4), is 1.5×10^{-8} g · cm⁻² · s⁻¹, whereas the measured linear rate constant is $k_l = 1.7 \times 10^{-5}$ g · cm⁻² · s⁻¹.



a

b

Fig. 7. Autoradiograph (a) and schematic drawing (b) of an iron specimen oxidized for 16 hr in natural dioxide and for 2 hr in labeled SO_2 .¹⁰



b

Fig. 8. Autoradiograph (a) and schematic drawing (b) of an iron specimen oxidized for 12 hr in natural sulfur dioxide and for 5 hr in labeled SO_2 .¹⁰

a

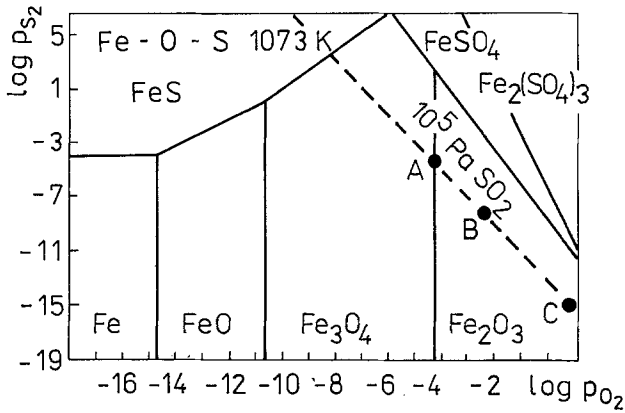


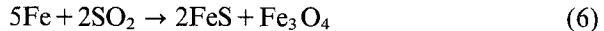
Fig. 9. Phase-stability diagram for the Fe-O-S system at 1073 K (data from Refs. 14, 15), (dashed line) the isobar for 10^5 Pa SO_2 , calculated using equilibrium (1). (A) pure SO_2 ; (B) SO_2 containing 10 Pa O_2 , taking into account reactions (1) and (2); (C) corresponding to the equilibrium of reaction (1).

$J(\text{O}_2 + \text{S}_2)$ is much smaller than the observed value of k_l . This means that these low partial pressures of S_2 and O_2 cannot justify the amount of oxide and sulfide formed on the scale surface. From the above considerations it follows that the process cannot proceed only by the reaction with O_2 and S_2 molecules, but rather by means of reaction (3).

Reaction (3) proceeds as long as the iron activity a_{Fe} on the surface of the scale is

$$a_{\text{Fe}} > P_{\text{SO}_2}^{-1/(2m+1)} \exp\left[\frac{\Delta G_3^\circ}{(2m+1)RT}\right] \quad (5)$$

The lowering of the iron activity at the scale-gas interface below the value established by Eq. (5) results in the growth of iron oxide as a thermodynamically stable phase. According to McAdam and Young,⁸ in the course of reaction (3) iron sulfide and magnetite are formed:



The required iron activity at 0.1 MPa of sulfur dioxide and 1073 K is $a_{\text{Fe}} > 1.8 \times 10^{-4}$ for reaction (6). On the surface of the metal ($a_{\text{Fe}} = 1$), $P_{\text{SO}_2} > 4 \times 10^{-5}$ Pa is sufficient for reaction (6) to take place.

The formation of an oxide layer starts after a few minutes. Further growth of the oxide-sulfide layer rapidly decreases and totally stops after 10 or so minutes. The second growth stage of this layer is very slow and takes place due to inward diffusion of sulfur or sulfur dioxide. Experiments

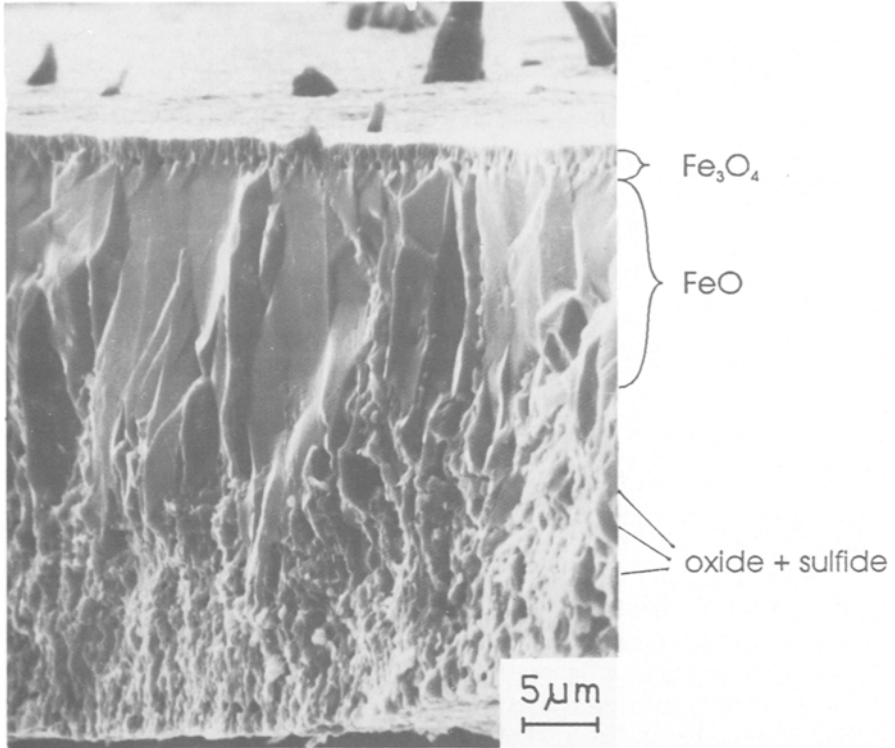


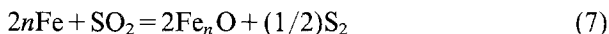
Fig. 10. SEM micrograph of the fractured scale formed after 40 min at 1073 K in $P_{\text{SO}_2} = 10^5$ Pa.

performed on the cobalt–sulfur–oxygen system at $P_{\text{SO}_2} = 3 \times 10^5$ Pa and iron–sulfur–oxygen at $P_{\text{SO}_2} = 3 \times 10^3$ Pa with the use of sulfur dioxide labeled with ^{18}O show the transport of sulfur dioxide molecules rather than sulfur and oxide.^{16,17} The morphology of our scale shows that sulfide also forms at oxide grain boundaries near the oxide–sulfide layer (Fig. 10).

As the oxide grains grow, the scale becomes more compact, and inward gas penetration practically ceases. The scale grows only at the scale–gas interface.

At a certain thickness, the scale separates from the core, initially at the corners and edges. According to the fissure-dissociation model,¹⁸ this process results in the formation of fissures facilitating inward gas transport (first at the corners), which was confirmed by the marker investigations.¹⁰ The penetrating sulfur takes part in the formation of the scale layer in the metal-consumption zone, first at the edges and after longer reaction times, over the whole sample (Figs. 7 and 8).

The formation mechanism of the oxide layer, which is the main part of the scale remains unexplained. The partial pressure of oxygen (from Eq. (1)) exceeds the dissociation pressure of each of the iron oxides, but the flux of oxygen molecules (calculated using Eq. (4)) colliding with the sample surface does not guarantee the observed instantaneous reaction rate during the parabolic process.⁶ Thus, the oxide-layer growth may be explained by Eq. (7):



The sulfur dioxide used in our experiments contained 10⁻²⁰% oxygen, and the calculated value of $J(\text{O}_2)$ was higher than the observed instantaneous reaction rates. Hence we conclude that the iron may react not only with sulfur dioxide but also with oxygen molecules at the scale-gas interface. Sulfur deposition on the cold parts of our apparatus, previously¹ observed, also indicates the sulfur dioxide reaction (7) with the liberation of sulfur.

Radiotracer studies of the nickel-oxygen-sulfur system¹⁹ have indicated that besides an inward transport of SO_2 sulfur transport in the opposite direction can also take place. This is due to a transformation of sulfide (unstable under the conditions of the process) into an oxide by reaction with oxygen or sulfur dioxide diffusing inward. To check whether a similar process occurs in the iron-oxygen-sulfur system, an iron sample has been oxidized first in sulfur dioxide labeled with sulfur-35 and then in the natural sulfur dioxide. No sulfur diffusion toward the scale-gas interface has been observed. This may be due to a number of causes:

- (a) The process is too slow to be observed during the experiment.
- (b) The liberated sulfur diffuses inward, and its transport could not be observed in the radioactive part of the scale.
- (c) The pressure of oxygen and sulfur dioxide in the inner part of the scale is too low for transformation of sulfide into oxide to take place, since the inward penetration of gas practically ceases.

CONCLUSIONS

1. Iron oxidation in sulfur dioxide takes place mainly due to outward diffusion of metal.
2. During the initial stage, when the iron activity at the scale-gas interface is high, iron reacts with sulfur dioxide to form an oxide-sulfide layer.
3. A compact oxide layer grows during the second stage of the process (after about 10 min) by iron diffusion to the scale-gas interface and reacting with sulfur dioxide and oxygen.

4. The formation of the oxide-sulfur layer is a linear rate process, whereas the oxide-layer growth follows a parabolic law.
5. Inward transport of SO₂ gas does not significantly affect the process.

REFERENCES

1. F. Flatley and B. Birks, *J. Iron Steel Inst.* **209**, 523 (1971).
2. N. Birks, in *Proc. Int. Symp. Properties of High Temp. Alloys* (Electrochem. Soc., 1976), p. 125.
3. A. Rahmel, *Corrosion Sci.* **13**, 125 (1973).
4. A. Rahmel, *Oxid. Met.* **9**, 401 (1974).
5. N. F. Chu and A. Rahmel, *Rev. High Temp. Mat.* **4(2)** (1979).
6. F. Gesmundo, *Oxid. Met.* **13(3)** (1979).
7. F. Gesmundo, C. de Asmundis, S. Merlo, and C. Bottino, *Werkstoffe und Korrosion* **30**, 179-185 (1979).
8. G. McAdam and D. J. Young, *Oxid. Met.* **28**, 165 (1986).
9. B. Chatterjee and A. J. Dowell, *Corrosion Sci.* **15**, 639 (1975).
10. J. Gilewicz-Wolter, *Oxid. Met.* **11**, 2 (1977).
11. K. L. Luthra and W. L. Worrell, *Metall. Trans.* **10A**, 621 (1979).
12. K. L. Luthra and W. L. Worrell, *Metall. Trans.* **9A**, 1055 (1978).
13. S. Mrowec and T. Werber, *Chemia Analityczna* **7**, 605 (1962).
14. I. Barin and O. Knacke, *Thermochemical Properties of Inorganic Substances* (Springer-Verlag, Berlin 1973 and Suppl. 1977).
15. *JANAF Thermochemical Tables* (Dow Chemical Co., Midland, Michigan, 1971).
16. J. Gilewicz-Wolter and K. Kowalska, *Oxid. Met.* **22**, 101 (1984).
17. J. Gilewicz-Wolter, *Bull. Acad. Polon. Sci. Ser. Chim.* **33**, 53 (1985).
18. A. Brückman, S. Mrowec, and T. Werber, *Fiz. Miet. Metallow.* **15**, 363 (1963).
19. J. Gilewicz-Wolter, *Oxid. Met.* **29**, 225 (1988).
20. A. Rahmel, *Werkstoffe und Korrosion* **23**, 272 (1972).